Shallow Geothermal Potential of the Snake River Plain

Joseph Batir[1], Maria Richards[1], Matthew Hornbach[1], David Blackwell[1], Amanda Kolker[2], and Al Waibel[3]

[1]Roy M. Huffington Department of Earth Sciences, Southern Methodist University, Dallas, Texas

[2]National Renewable Energy Laboratory, Golden, Colorado

[3]Columbia Geoscience, Portland, Oregon

Keywords

Snake River Plain, EGS, temperature-at-depth, Oil and Gas wells, Radiogenic Heat Production,

ABSTRACT

The Snake River Plain (SRP) terrestrial heat flow and subsurface thermal regime are not well understood but are important for assessing the local geothermal resource potential, both for conventional and for Enhanced Geothermal Systems (EGS) development in the region. Resource evaluation for the SRP is complicated by the disparate data density, along with the known lateral advection of heat in the Eastern Snake River Plain Aquifer and vertical heat transport by fluids in the bounding faults, primarily in the southwestern section. Fortunately, recent studies, e.g., the Snake River Plain Play Fairway Analysis, the Idaho FORGE site, and site-specific investigations, which included drilling within the Camas Prairie and on the Mountain Home Air Force Base, near Twin Falls, and in the Eastern Snake River Plain as part of the *HOTSPOT* Project, add both additional drilling and geophysical data. The SMU Geothermal Laboratory has conducted detailed studies of SRP tectonics and heat flow since the 1970's and used this knowledge as part of the EGS geothermal potential estimation for the conterminous United States in 2006 and again in 2011, calculating geothermal potential from 3.5 km to 10 km depth. Recent temperature modeling refined the calculation methodology to estimate shallow (1 km to 4 km) resource potential using an improved thermal conductivity model and incorporation of shallow groundwater flow. By incorporating the new SRP geology, geophysics, and 206 thermal data sites into the SMU thermal modeling methodology, this project updates the resource estimate for the SRP, and generates new temperature-at-depth maps for the shallow subsurface (1 km to 4 km). The project results highlight the EGS potential resource areas (≥150°C) and areas with more exploration risks based on minimal and/or low-quality data. The newest temperature modeling results suggest EGS potential is near five times greater in the SRP than previously estimated.

1. Introduction

The Snake River Plain (SRP), part of the Yellowstone hotspot track, has been a target for geothermal energy production for nearly 50 years. Previous research studied the broader thermal regime for southern Idaho and its interactions with the hydrological regime across the SRP and more specifically the Eastern Snake River Plain Aquifer (ESRPA) (Blackwell, 1969; Blackwell, 1971; Brott et al., 1976; Brott et al., 1978; Brott et al., 1981; Blackwell, 1989; Blackwell et al., 1992; McLing et al., 2016). Early studies collected small regional data for geothermal exploration including areas in central Idaho, near known Idaho batholith hot springs, the Eastern Snake River Plain (ESRP), Camas Prairie, Owyhee Plateau, Grandview, Rexburg/St. Anthony/Teton River, Weiser, and others (Blackwell, 1969; Blackwell, 1971; Brott et al., 1976; Brott et al., 1978; Brott et al., 1981; Blackwell, 1989; Blackwell et al., 1992). These works were a collaboration of industry exploration, fundamental research, and early-stage exploration driven research.

Much of the shallow thermal regime is characterized by high ground flows (up to 1 km/yr in the ESRPA and artesian flow of 0 to 40+ gal/min in wells throughout the SRP) in local to regional aquifers. Consequently, geothermal energy production in the SRP will likely be realized through the utilization of Enhanced Geothermal Systems (EGS). This study provides insight into the thermal regime of the upper 1 to 4 km of the SRP, with specific interest in temperatures over 150 °C for future EGS exploration and development, by utilizing the most recent temperature calculation methodology combined with reevaluation of new and old temperature data, an updated thermal conductivity model, and geologic and geophysical subsurface crustal models. This effort builds from a series of works that improved the methodology and tools for broad-scale heat flow and temperature-at-depth mapping which produce higher resolution results by estimating heat flow and temperatures for every data point location with detailed temperature and thermal conductivity models (Blackwell et al., 2006; Blackwell et al., 2011b; Stutz et al., 2012; Frone et al., 2015; Jordan et al., 2016; Smith, 2016; Smith and Horowitz, 2016). As part of this project, the model steps do not change, rather the data input is refined based on availability to data that represent the deep regional thermal regime.

The most recent geothermal projects in the SRP include the SRP Play Fairway Analysis (Shervais et al., 2020), the Idaho Frontier Observatory for Research in Geothermal Energy (FORGE) project (McCurry et al., 2016; Podgorney et al., 2016), and the *HOTSPOT* Drilling Project (Shervais et al., 2012). The recent studies add geological and geophysical understanding and provide opportunities for comparison in Camas Prairie (Glen et al., 2017; 2018; Shervais et al., 2020), Mountain Home (Lachmar et al., 2019), and in the ESRP at the 2010 drilled Kimama well. This project increases the knowledge of the deeper thermal regime through the addition of deep (700 – 4000 m) oil and gas wells, new geothermal wells, and reassessment of heat flow data (well temperature gradients, thermal conductivities based on rock cores or lithology, and radiogenic heat production of actual samples and predicted values). Other relevant data are also examined including Quaternary fault lines, volcanic formation ages and locations, geological cross-sections, and review of previous results from gravity and magnetic maps that define aquifer thickness and interpreted lithologies (Whitehead, 1992; Lindholm, 1996). Improvements on past research include the updated thermal conductivity model and increased mitigation of error from groundwater flow in the thermal model (Blackwell, 1989; Blackwell et al., 1992).

The geothermal resource by its temperature component between 1 and 4 km is defined here for the first time utilizing additional temperature data, thermal conductivity, lithology, and crustal structure studies combined with the most recent heat flow and temperature-at-depth calculation methodology. The additional data increase the resolution and variability of temperature estimates, and the new temperature estimates make it possible to examine where EGS opportunities may occur in the region. The resulting temperature-at-depth maps and updated resource estimate for each 1 km depth thickness below the SRP highlight areas with the greatest EGS potential and highlight areas with the highest risk associated with sparse or low-quality data.

2. Snake River Plain Geology

The SRP is a physiographic region defined by the arcuate topographic low visible on elevation maps that formed in response to the interaction between the North American Plate and the Yellowstone hotspot. The SRP can be divided into three areas: the Western Snake River Plain (WSRP), Central Snake River Plain (CSRP), and the Eastern Snake River Plain (ESRP) (Figure 1). While they are different, all three subregions are thought to be related to the Yellowstone Hotspot. The detailed geologic history of the SRP is described by Wood and Clemens (2002), Shervais et al. (2002), and Pierce and Morgan (2009). The CSRP and ESRP can be described broadly as a series of young, small basaltic eruptions underlain by older felsic calderas. In this way it differs from the Columbia River Basalts to the west, which are thick and widespread flows. This difference is visible in temperature logs, with Columbia River Basalts exhibiting a stair stepping pattern associated with confined aquifers at the base and top of basalt flows that become connected in open-hole sections of a well (Blackwell et al., 1990; Frone et al., 2015). In contrast, temperature logs within SRP basalts show a large isothermal zone throughout the section because the thin basalt flows do not confine aquifer flow. The WSRP formed as a rift style basin through lithospheric weakening from the passing Yellowstone Hotspot (Wood and Clemens, 2002). Lacustrine sediment packages are interbedded between basalt flows in the WSRP (Wood and Clemens, 2002). Various exploratory drilling penetrates felsic rock on the margins of the WSRP, but the deepest wells in the center of the basin do not intersect felsic rocks.

Studies in the Cascade Range, Columbia Plateau, and Snake River Plain clearly show that basalt permeability relates to degree of alteration (Bargar and Keith, 1999; McLing et al., 2016; Frone et al., 2016; Lachmar et al., 2017). High temperature alteration or prolonged low temperature groundwater flow that leads to mineral precipitation reduces permeability in basalt pore space and fracture zones, which inhibits groundwater flow and establishes a conductive thermal regime. We observe evidence for these same phenomena in the ESRP (Whitehead,1992 & Lindholm,1996), and may exist at other sites, including the Kimama drill hole in the ESRP (Lachmar et al., 2017) and in drilling at Newberry Caldera (Bargar and Keith, 1999). Hence in the SRP basalt aquifer the thermal regime tends to be isothermal throughout the thickness of the aquifer from high flow rates through the connected pore and fracture permeability (see temperature log examples in McLing et al., 2016), while in the Cascade Range and Columbia Plateau, heat flow may be conductive over much of a system of confined aquifers. The

domination of lateral and vertical convective flow in the SRP in the top 100+ meters means that only wells that completely penetrate these flow zones may give useful thermal information.

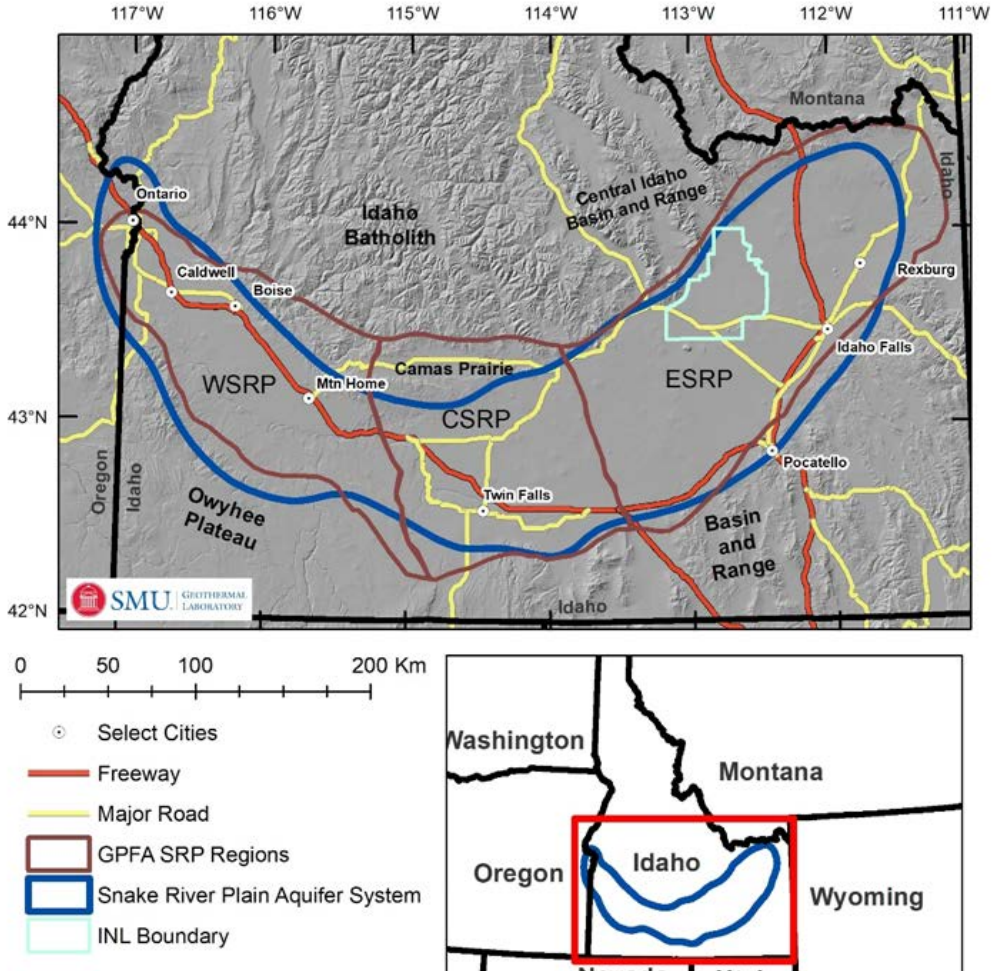

Figure 1: The Snake River Plain region of Idaho and Eastern Oregon. The study area is defined by the USGS as the Snake River Plain Aquifer System, the blue outline. The recent Geothermal Play Fairway Analysis defined the Snake River Plain slightly differently, following the brown outline.

Faults were also used in the SRP Geothermal Play Fairway Analysis (GPFA) as a potential indicator for geothermal power potential, specifically as an indicator for higher permeability (Shervais et al., 2015; Shervais et al., 2020). There are two primary regional fault trends that crosscut the SRP. The WSRP has a WNW trending fault system associated with formation of the sag and graben WSRP basin. This fault trend is young, Miocene to Quaternary aged and bounds the northern and southern boundaries of the WSRP (Ludington et al., 2005; Machette et al., 2003; Wood and Clemens, 2002). These faults are high angle with fault motion mostly normal with some minor oblique to strike slip movement. Previous work highlights the WNW fault trend as a primary permeability target for geothermal exploration because of the age, density, and slip tendency of these faults (DeAngelo et al., 2016; Shervais et al., 2020). The second regional fault trend strikes NNW to N and encompasses much of the area surrounding the SRP and is

hypothesized to underlie the ESRP (Rodgers et al., 2002). This fault group is primarily older, but contains some Quaternary faults, mostly north and southeast of the SRP. These faults are thought to underlie and account for extension of the ESRP as continuations of the range bounding faults visible both north and south of the ESRP (Rodgers et al., 2002). These faults could alternatively form through cooling related subsidence (Pierce and Morgan, 2009). In this study, the faults of most interest are Quaternary aged faults because the recent fault movement is hypothesized to have more potential for fluid flow, and with fluid flow would contain advective thermal signatures not representative of the regional conductive thermal regime.

3. Method, Model Inputs, and Data

The thermal model used here is the simplified steady-state one dimensional heat diffusion equation with additional radiogenic heat production to produce site-specific heat flow and temperature-at-depth calculations. The methodology uses an input of a thermal conductivity model and geothermal gradient data for each site to first calculate terrestrial heat flow, which then becomes the foundation to calculate the deeper temperatures-at-depth. Next, the new heat flow, thermal conductivity model, and assumed basement properties become inputs to calculate temperature to a given depth (Smith, 2016; Smith and Horowitz, 2016). We reevaluated and filtered available well data to remove advection influenced temperature data and incorporated geological and geophysical data to refine sediment thickness and stratigraphy for the site-specific thermal conductivity models. New geophysical studies are also used to define the thickness of the upper crust for radiogenic heat production. These changes improve the accuracy and resolution of the resulting temperature estimates and geothermal resource potential.

3.1. Model Parameters

For this study we incorporate surface temperature, temperature logs, bottom-hole temperature (BHT), lithology logs, thermal conductivity measurements, mapped aquifer temperature and thickness, upper crust thickness estimates from seismic studies, and previous regional cross sections to generate a new heat flow map gridded at 3’ by 3’ spacing. Data are examined so that the final maps are representative of the deep (>1.5 km), conductive, regional thermal regime. Specific input data utilized for the heat flow and temperature-at-depth calculation and how these differ from previous SRP resource estimations are discussed below.

3.1.1 Site Temperature and Heat Flow Data

Temperature data from equilibrium temperature logs and BHT are utilized to calculate geothermal gradient for heat flow calculations. New criteria are applied based on well temperature source being either an equilibrium temperature-depth log or a BHT measurement (Table 1) and then filtered based on maximum depth of temperature (Table 2). Temperature log data shallower than 125 m are eliminated to remove potential near surface influences not representative of the deeper thermal regime. BHT measurements shallower than 600 m are eliminated to minimize drilling disturbances following methods in Blackwell et al. (2010). A second level site-by-site filtering of the data removed additional sites with temperature measurements displaying localized temperature phenomena (i.e. an isothermal section or temperature overturn) that do not reflect the deeper (1 to 4 km) subsurface thermal regime.

Resulting available data are used to calculate the site geothermal gradient. Geothermal gradient is calculated from the deepest conductive zone for equilibrium temperature logs, or from surface to depth of BHT for BHT only wells, utilizing near surface water temperature from Gass (1982) as the surface temperature. With all these filtering criteria incorporated, there is a reduction in the southern Idaho dataset from 933 to 207 data points (Figure 2). New temperature data include 74 BHT measurements and 2 temperature-depth logs, which is approximately 40% of the temperature data. The 207 point temperature data set improves upon previous work in that the temperature gradients are all interpreted to represent the deep regional thermal regime.

Table 1. Temperature data Selection Criteria.

Temperature Measurement Type	*Specific Criteria for Well Site Inclusion in Study.*
Temperature-Depth Log	• Deeper than 125 m • Conductive, linear gradient if at bottom of well log (convection/isothermal section okay if not deepest section) • Bottom depth not within a known geothermal system well (e.g. Boise, Camas Prairie – Magic Reservoir, Rexburg)
Bottom Hole Temperature (BHT)	• Deeper than or equal to 600 m • BHT value as compared to other surrounding data indicates a linear gradient

Table 2. Well Temperature Data Distribution by Depth

Depth	**Number of Sites**	**Number of Sites used**	**Percentage of Original Data**
Near Surface (<125 m)	490	0	0%
Shallow (125 – 600 m)	245	142	26%
Medium (> 600 m)	84	50	9%
Deep (> 1000 m)	114	57	12%

Compilation of the terrestrial heat flow data includes: 1) the SMU Geothermal Laboratory heat flow data on the National Geothermal Data System (NGDS), 2) the related SMU temperature-depth well logs for the southern Idaho and eastern Oregon, 3) the Idaho Geologic Survey borehole temperature content-model dataset, 4) new temperature-depth well logs associated with the project *HOTSPOT* (Utah State University, 2014a; 2014b; 2014c) and 5) Idaho oil and gas exploration well lithology and temperature data collected for this project from 24 Idaho sites drilled after 2007 (sites newer than current upload in the Idaho Geologic Survey data collection for the NGDS (Figure 2). The Oregon Department of Geology and Mineral Industries borehole temperature content-model and online geothermal well database (GTILO-2_Geothermalwell_database.xls) were examined for additional new data.

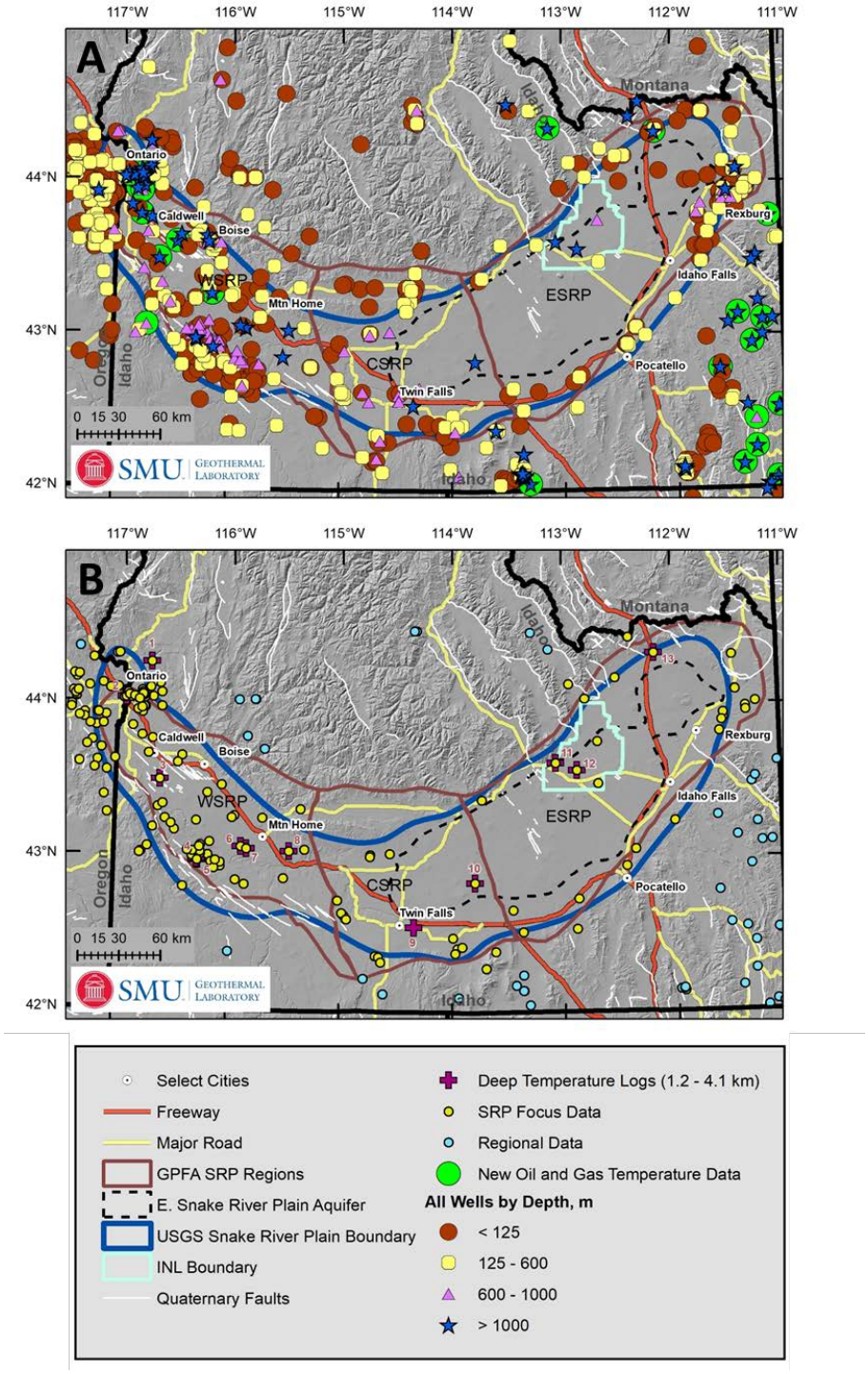

Figure 2. (A) Temperature points plotted by depth of bottom temperature measurement. Note that there are more than 933 points on this figure because of wells with multiple temperature values. At locations with multiple heat flow values, the value with the highest confidence is used for further calculations. (B) Data in southern Idaho that pass all data filtering criteria. These data record the deep thermal regime and are used for temperature-at-depth and resource potential calculations. Data within 20 km of the USGS Snake River Plain Boundary are the yellow data and data outside this 20 km buffer are the light blue dots. The regional data are included in interpolation to minimize boundary interpretation errors within the Snake River Plain.

3.1.2 Geology, Lithology, and the Thermal Conductivity Model

A thermal conductivity model is constructed for each site and used in calculating the terrestrial heat flow and extrapolating temperature to given depths. The generalized stratigraphic column total thickness is set equal to the depth to basement and individual stratigraphic bed thicknesses are uniformly scaled to fit the new total column thickness, while conserving percent thickness of each formation. This site-specific stratigraphic column, with estimated thermal conductivity of each stratigraphy intersected, is then used to calculate a depth and thickness weighted thermal conductivity, which is used for heat flow and/or temperature-at-depth calculations (Blackwell et al., 2010; Smith and Horowitz, 2016). Each site is assigned a site average value using this process. Only measured thermal conductivities within the SRP are utilized for constructing the thermal conductivity model. While only using SRP measured values increases potential error because of a low sample size, this method is preferred because measured values are coming directly from the study area and are therefore more representative.

Table 3. Assigned thermal conductivities based on rock type.

Volcanic Rocks		**Sedimentary Rocks**	
Rock Type	**Volcanic Thermal Conductivity, $Wm^{-1}K^{-1}$**	**Rock Type**	**Sediment Thermal Conductivity, $Wm^{-1}K^{-1}$**
Rhyolite	1.75	**Shale**	1.2
Basalt	1.3 – 2.0	**Sandstone**	2.0
General Volcanics*	1.4 – 1.5	**Interbedded Sandstone / Shale**	1.9
Interbedded Basalt / Shale	1.4 – 1.6	**Interbedded Siltstone/Sandstone**	1.7
Interbedded Basalt / Sediments	1.5	**Limestone**	2.3
Interbedded Rhyolite / Basalt / Sediments	1.7	**Interbedded Shale/Limestone**	1.9
		Interbedded Limestone/Sandstone	2..4
		General Sedimentary	1.7 - 1.9
Basement Conductivity (Average of Felsic Rocks)		2.3	

*General volcanics is assigned when original lithology logs did not indicate details on the thickness or percentages of respective volcanics in a section, providing no quantitative way to calculate a percent weighted thermal conductivity.

Sedimentary rock thermal conductivity is assigned based on the site sedimentary rock types and related values from WSRP wells ORE-IDA 1, VALE 47-10, and Anschutz (Brott et al., 1976; NGDS, 2014), and thermal conductivity for the basalt and rhyolitic rocks are assigned from measured values from the closest applicable measured value (Table 3) (Blackwell, 1989; Blackwell et al., 1992; Shervais et al., 2012; Shervais et al., 2013; Lachmar et al., 2017; Lachmar et al., 2019). New measurements for basalt and rhyolite come from the *HOTSPOT* wells (Shervais et al., 2012; Lachmar et al., 2017; Lachmar et al., 2019). A thermal conductivity model is produced using measured values. This model is variable but generally decreases with

increasing depth, based on the nearest equivalent depth measured thermal conductivity value. This decreasing thermal conductivity with increasing depth matches the Frone et al. (2015) thermal conductivity model that also decreased with increasing depth that used a thermal conductivity – temperature relationship. This study improves the thermal conductivity portion of heat flow calculations for the SRP by being the first to incorporate the site-specific depth and stratigraphy correlated thermal conductivity models as opposed to a single estimated thermal conductivity based on drilling reports or cuttings piles (Blackwell, 1989).

Compilation of the lithology data included the Idaho lithology interval content model uploaded to the NGDS (Idaho Geologic Survey, 2013), individual oil and gas, geothermal, and water wells deeper than 1000 ft (305 m) from Idaho and Oregon, well logs from the Idaho National Laboratory (INL) FORGE project (Podgorney et al., 2016), and new lithology from the three *HOTSPOT* drilling project wells (Shervais et al., 2012; Shervais et al., 2013) (Figure 3). Wells are manually examined and used to construct generalized lithology sections for the WSRP, CSRP, and ESRP with estimated variability within the thickness of a given lithology section (see Final Report Appendix in Batir et al., 2020b). Aquifer thickness was estimated using electrical resistivity and is interpreted as the depth to the hydrothermally altered basalt and/or clay filled low porosity section (Whitehead, 1992; Lindholm, 1996). The lithology within the ESRPA was interpreted as unaltered basalt.

3.1.4 Basement Parameters and Radiogenic Heat Production Model

In addition to the heat flow value and thermal conductivity model at each point, the temperature-at-depth calculation requires inputs for basement thermal conductivity, mantle heat flow (Q_m), and thickness of the radiogenic heat producing layer (*b*) (attributed to the felsic upper crust). Inputting those values provides an estimate of the radiogenic heat production (A) contribution to the measured terrestrial heat flow (Q) (Smith, 2016; Smith and Horowitz, 2016). Basement thermal conductivity is assigned 2.3 W/m*K as the average of felsic rocks within the SRP (Brott et al., 1976; Blackwell, 1989; Blackwell et al., 1992; Kimberly, unpublished values) and Q_m is set to 60 mW/m² (Roy et al., 1968). The *b* value is assigned based on sediment thickness. If sediment thickness is less than 3 km, *b* is set to 7.5 km; if sediment thickness is greater than 3 km, *b* is calculated as 10.5 km – sediment thickness. This *b* assignment incorporates new upper crust thickness estimates beneath the SRP (Hill and Pakiser, 1967; Sparlin, 1981; Harper, 2018) and uses the *b* calculation methodology from Blackwell et al. (2007), Blackwell et al. (2010), Smith (2016), and Smith and Horowitz (2016). The A value is calculated at each site to satisfy the Q-A relationship described by Roy et al. (1968) and Lachenbruch (1968). This calculation assumes that all other inputs into the model (Q, Q_m, and *b*) are correct, which then calculates an A value to force the Q-A relationship to be true. This heat production model improves the SRP thermal regime modeling by utilizing the recent work of Harper (2018) to re-define the *b* layer thickness and calculates site specific A values so that the Q-A relationship is satisfied at all data locations.

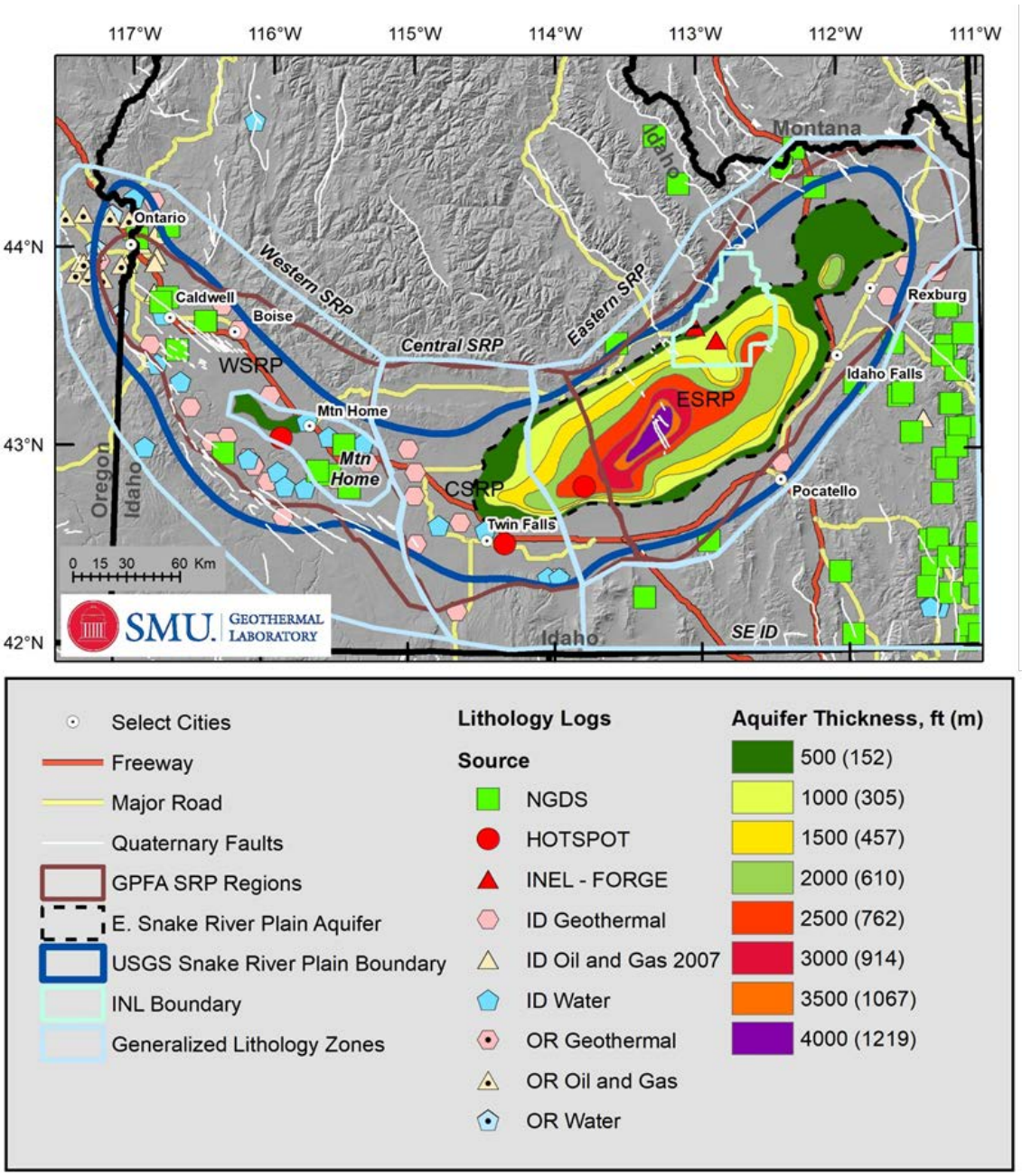

Figure 3. Data used to produce the 5 generalized thermal conductivity models for the SRP. Thermal conductivity model areas include: Western Snake River Plain, Mountain Home, Central Snake River Plain, Eastern Snake River Plain, and SE ID, which is the area southeast of the Snake River Plain. The Eastern Snake River Plain Aquifer thickness is utilized to estimate basalt thickness and as a temperature-depth input. The lithology columns are available in the related Final Report Appendices (Batir et al., 2020b).

3.2. Data Density, Contouring Control, and Gridding

Heat flow, as the primary data source, and subsequently temperature-at-depth data sites, define the data density and appropriate grid size for mapping. The accuracy of the heat flow and temperature-at-depth maps is directly related to the density of the data and the geologic/geophysical constraints in the model for areas without any data. Areas in the ESRP with few or no data points incorporate the aquifer depth contours to aid in defining depth to the conductive thermal regime as a way to increase the accuracy of mapping this region that has low data density.

The heat flow map is gridded in ArcGIS using Spline with a smoothing factor of 1. Gridding is performed at a more refined grid (3' Latitude/Longitude) than past analysis, allowing for more inclusion of site data values. Data density is still low for the ESRP, but new data in the WSRP have increased data density and now most of the WSRP portion of the heat flow map contains at least one data point within any 15 km radius circle (Figure 3). This heat flow map of the SRP overall has less data, yet by removal of near surface data and temperature logs with fluid flow, the results are more representative of the deep thermal regime for geothermal resource exploration.

4. Results

Surface heat flow values, temperature-at-depth calculations, and a percent difference of the modeled versus observed temperatures are presented as maps for the SRP region along with the regional data (Figures 5 – 10). The heat flow map is based on the newest heat flow determination for the SRP which utilizes the 207 data points considered to be representative of the regional thermal regime. Based on the heat flow, the thermal modeling outputs the resulting temperatures, which are mapped in 25 °C increments from 100 °C to 250+ °C for consistency in mapping the EGS resource potential. The current EGS electricity production potential values are calculated with a temperature cutoff of 150 °C, yet temperature maps display temperatures to 100 °C for future reference as improvements are made and lower temperatures can be economically utilized for power production. Additionally, the high temperature contouring is limited to 250+ °C to limit gridding in areas of sparse data, and to not over-emphasize regions of high extrapolated temperatures. The equilibrium temperature measurement in the Bostic 1A well is 188 °C at 2.7 km with a gradient of 66 °C/km, which extrapolates to 274 °C at 4 km, agreeing with model temperature estimates (Batir et al., 2020b, see Appendix for site details). While these extrapolated temperatures agree with observed temperatures where available at shallower depths, all extrapolated temperatures are inherently higher risk because of the lack of direct observation.

In general, the ESRP has higher heat flow than the WSRP, although this comparison is biased by data distribution. There are approximately 90 data sites within the WSRP, 16 in the CSRP, and 17 in the ESRP. Wells in the CSRP and ESRP are primarily located along the SRP margins, whereas the WSRP contains a more even distribution of data between the margins and SRP central axis. Temperature distribution is variable. The CSRP and WSRP contains a variable temperature distribution tied to spatial data location. The ESRP contains primarily higher temperature estimates except for a large low temperature region from the southeast border of INL property, north to Rexburg, and southeast to approximately 25 km northeast of Pocatello.

This low is driven by one lower heat flow point and the presence of the ESRPA. Similarly, the high temperature region in the western part of the ESRP is interpolated from the Kimama well. While these are high quality data and show a conductive, linear gradient below the ESRPA, interpolation for this large area is controlled by a low number of data points and need further study.

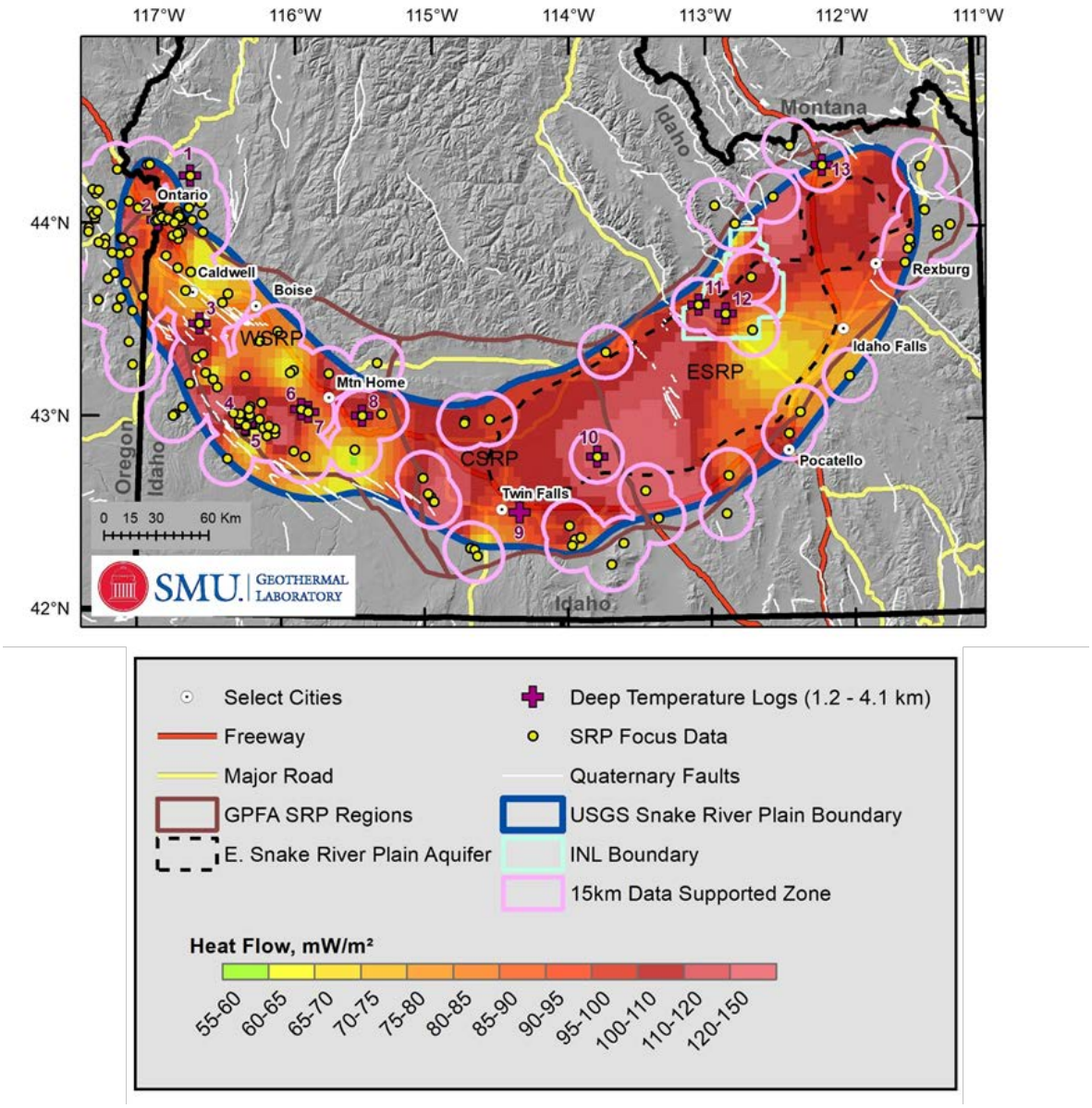

Figure 4. Terrestrial heat flow and data coverage map. Areas within the light pink outline have a minimum of one data point within a 15 km radius. Much of the WSRP is data supported, whereas much of the CSRP and ESRP have low data coverage. Deep Temperature logs are displayed, showing where there are direct temperature observations to modeled depths. Temperature logs correlate to numbers in all figures as follows: 1 = RDH-CHA #1, 2 = ORE-IDA #1, 3 = Upper Deer Flat #11-19, 4 = Federal #60-13, 5 = Lawrence D. #1, 6 = MTH #2B, 7 = Mt. Home AFB #1, 8 = Bostic #1-A, 9 = Kimberly (KMB), 10 = Kimama (KMA), 11 = INEL-GTL1, 12 = INEL-WO2, 13 = Hagenbarth #22-25.

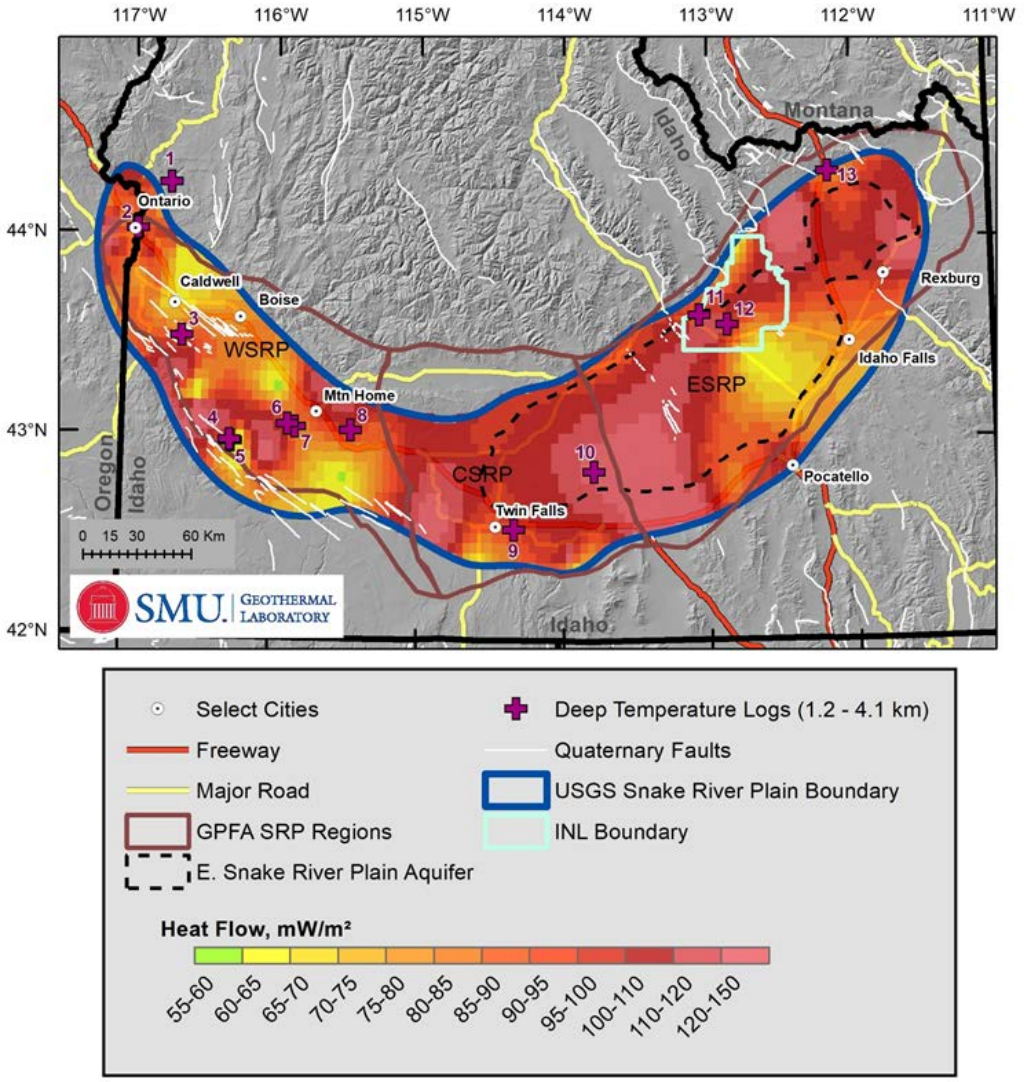

Figure 5: Terrestrial Heat Flow of the Snake River Plain. There is generally high heat flow in the range of 90 – 150 mW/m² with some select zones of heat flow in the 55 – 60 mW/m² range.

We assess potential uncertainty in the temperature maps by comparing measured BHT to the modeled BHT for wells greater than 750 m as a BHT percent difference map (Figure 10). The measured BHT is subtracted from the modeled BHT and calculated as a percentage on the measured BHT to determine a percent error in calculating measured BHT. A negative percent error means the modeled temperature is less than the measured and the thermal model is underpredicting the measured temperature value. A positive percent error means modeled temperature is greater than the measured and the thermal model is overpredicting the measured temperature value. Most wells have a modeled temperature within 10% of the measured temperature. Since most of the deep temperature measurements are oil and gas BHT measurements, 10% is within the error of temperature measurement and shows the modeled temperatures are in good agreement with measured temperature values. There are several underpredicted temperature values. One well near the Vale geothermal anomaly in the far

western WSRP is underpredicted by 20 to 30%. This area is a known geothermal anomaly, although temperature logs from this anomaly were included in mapping because they display a conductive, linear gradient. Similarly, wells near the Rexburg geothermal anomaly in the ESRP and wells near Mountain Home are underpredicted by 10 to 20% The Rexburg area is another known geothermal anomaly, and the Mountain Home region contains a potential geothermal resource (Lachmar et al., 2019). These underprediction areas suggest the temperature model is best suited for regional thermal mapping and underpredicts known geothermal resource areas. This is expected because the local thermal regime of a geothermal anomaly will be hotter than the background thermal regime, which is preferentially predicted by the temperature modeling. We consider this a conservative resource estimation model because deep temperature estimates which are incorrectly predicted are less than the measured temperature. This model, therefore, errors on the side of underprediction as opposed to overprediction of potential resource.

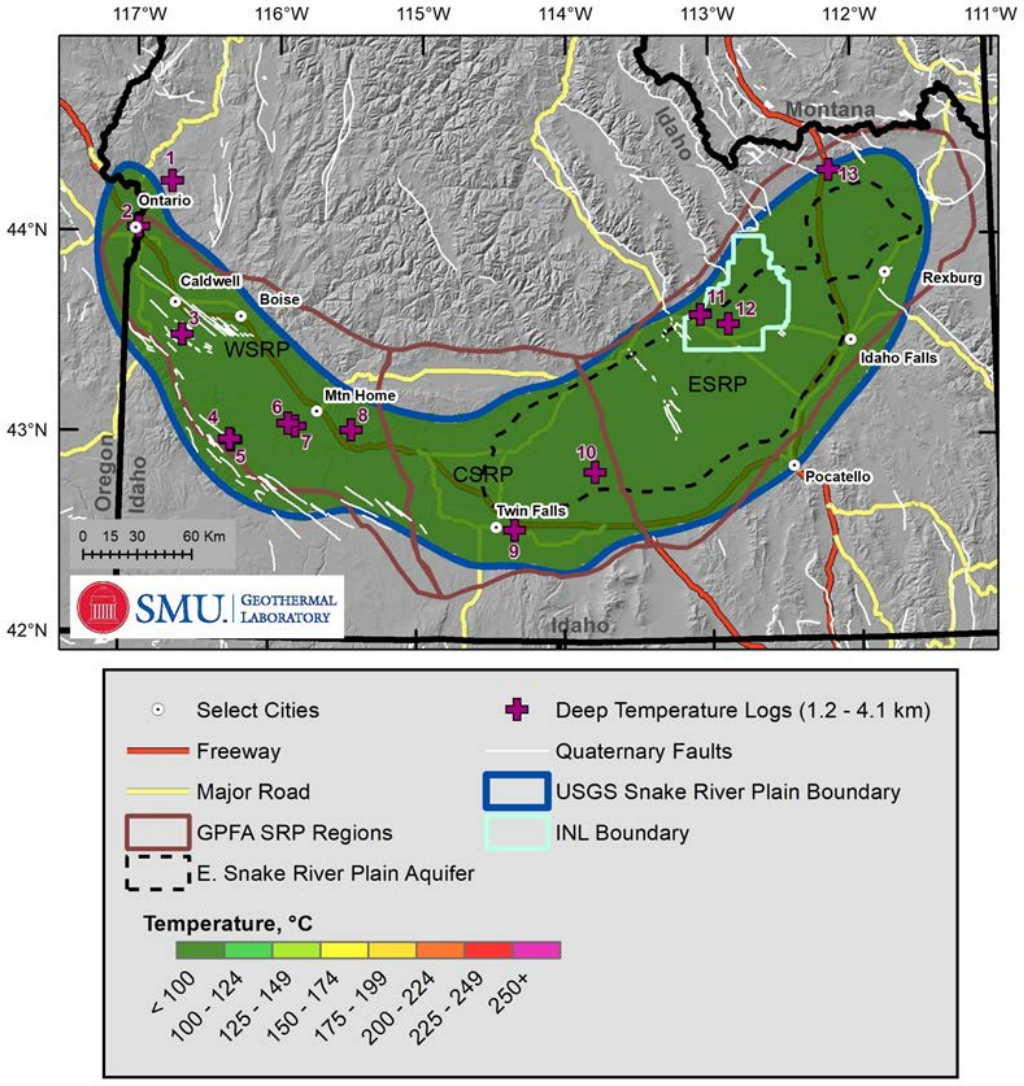

Figure 6: Estimated temperature at 1 km depth. The entire Snake River Plain region is below 100 °C at this depth, which is below the EGS electricity production lower limit of 150 °C. While the temperatures preclude EGS development, there is potential for conventional uses of lower-temperature geothermal fluids (e.g., direct use of the thermal resource for heating applications).

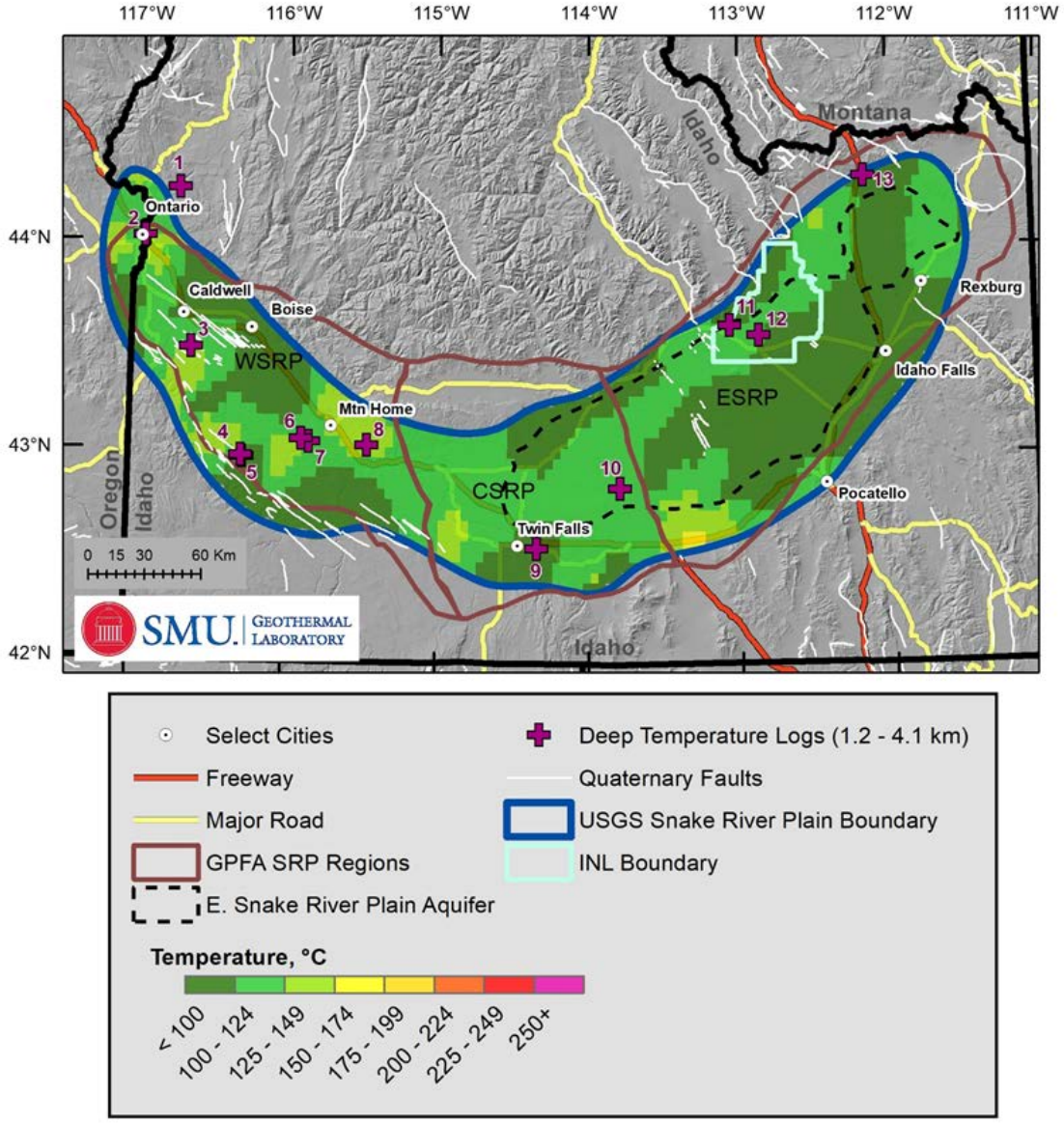

Figure 7: Estimated temperature at 2 km depth. Temperatures are generally higher than at 1 km depth, although some zones are still less than 100 °C. Areas with temperature less than 100 °C roughly align with surface outcrops of volcanic rocks and a resulting thin layer of sediment cover. There are several areas at 2 km depth with estimated temperatures of 150 °C or greater (yellow squares). Those are designated as areas with EGS potential. Most of these zones are interpolations and not directly measured temperatures. Any area not directly tied to measured temperature should be interpreted as requiring more information and additional drilling to confirm resource for high temperatures areas and eliminating an area as too cold to be a resource.

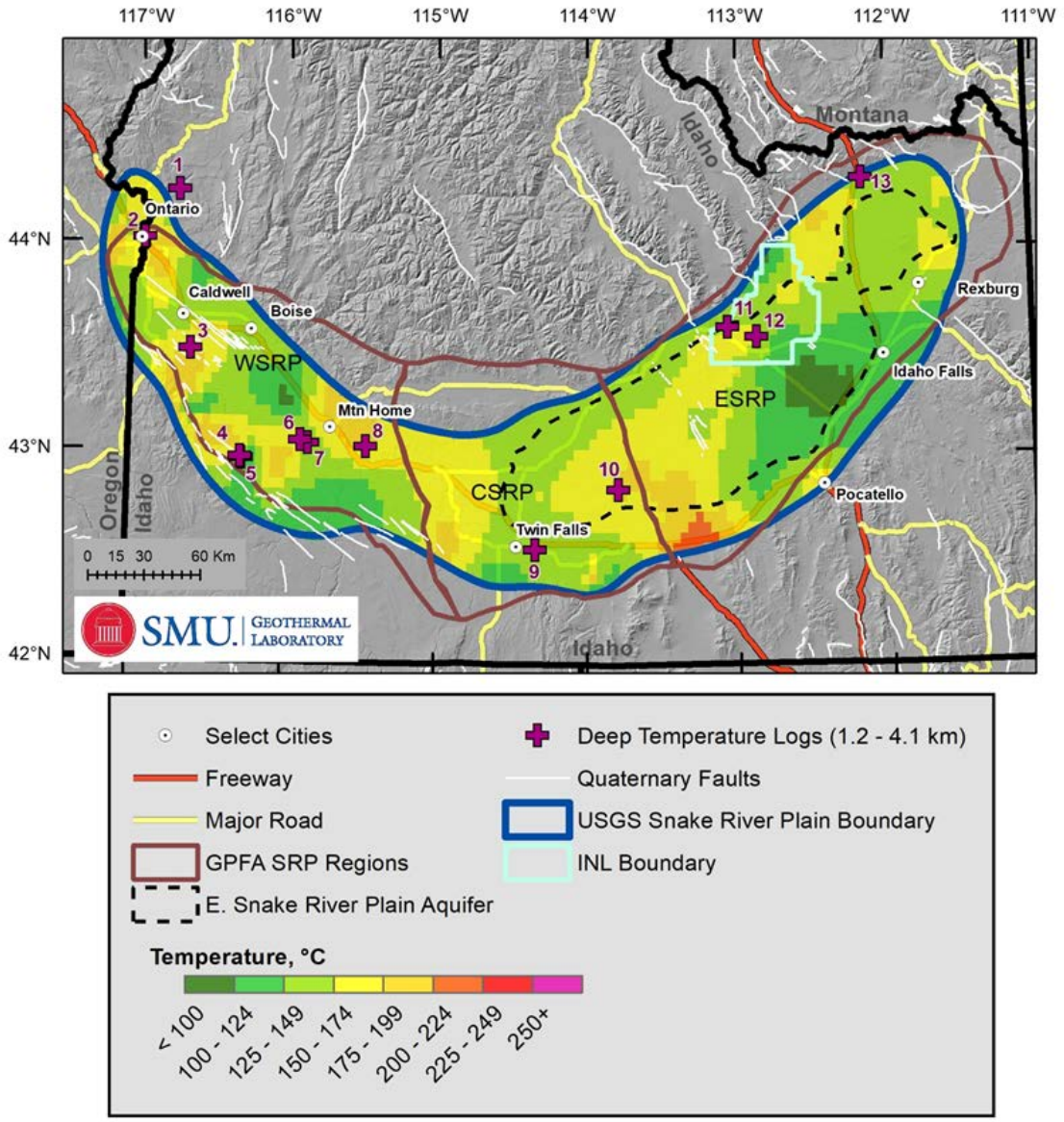

Figure 8: Estimated temperature at 3 km. Similar patterns of temperature are visible as seen in the 2 km temperature map. The same higher temperature areas at 2 km are locations calculated at this depth to be greater than or near 200 °C (orange to pink colors). These high temperature values may be the result of surface heat flow measurements associated with a shallow (upper 500 to 1000 m) thermal anomaly.

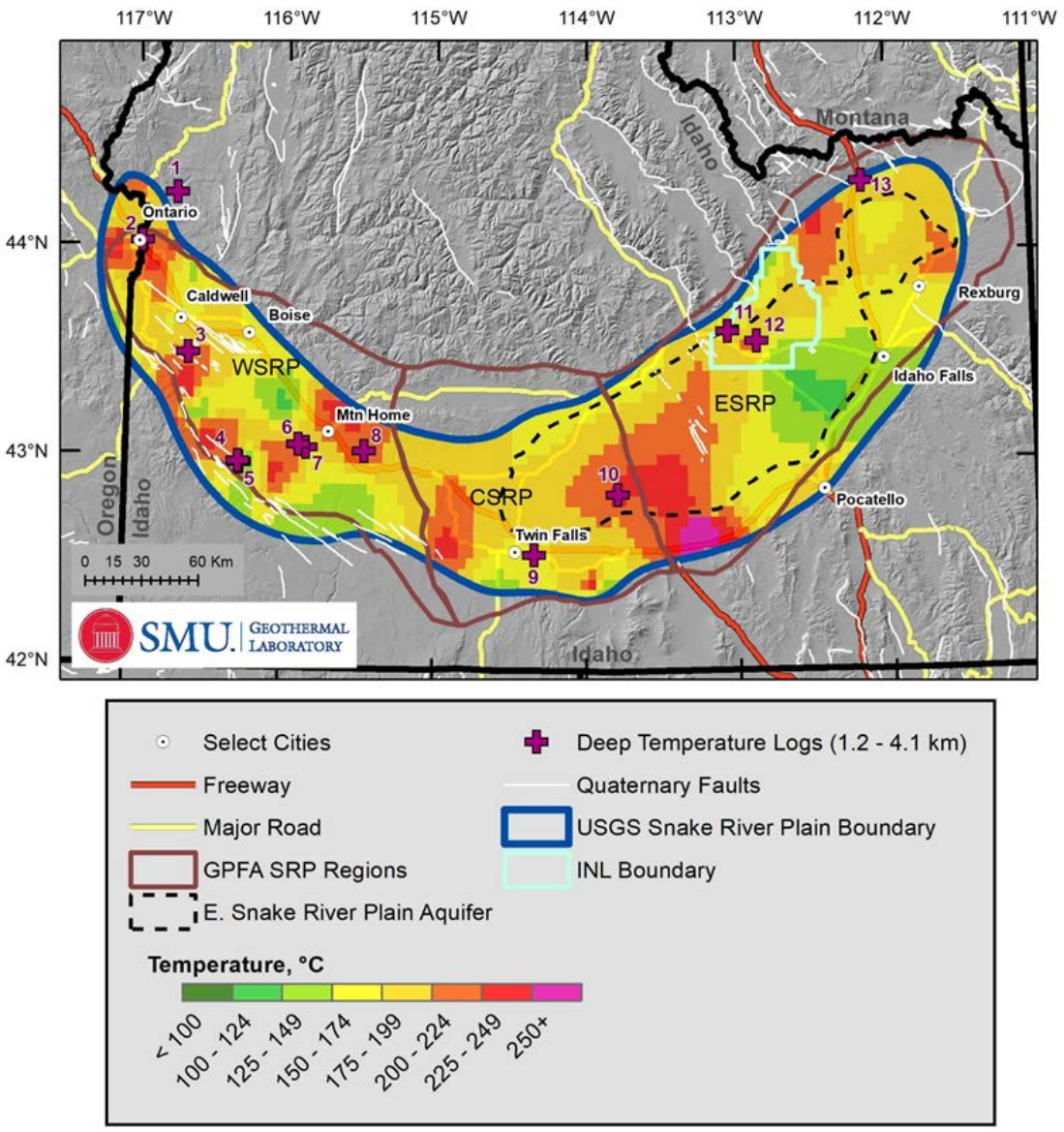

Figure 9: Estimated temperature at 4 km. Large sections of the Snake River Plain are predicted to be at a temperature capable of producing electricity at 4 km depth. High temperature regions at this depth require further examination through drilling and/or additional geophysical/geochemical work.

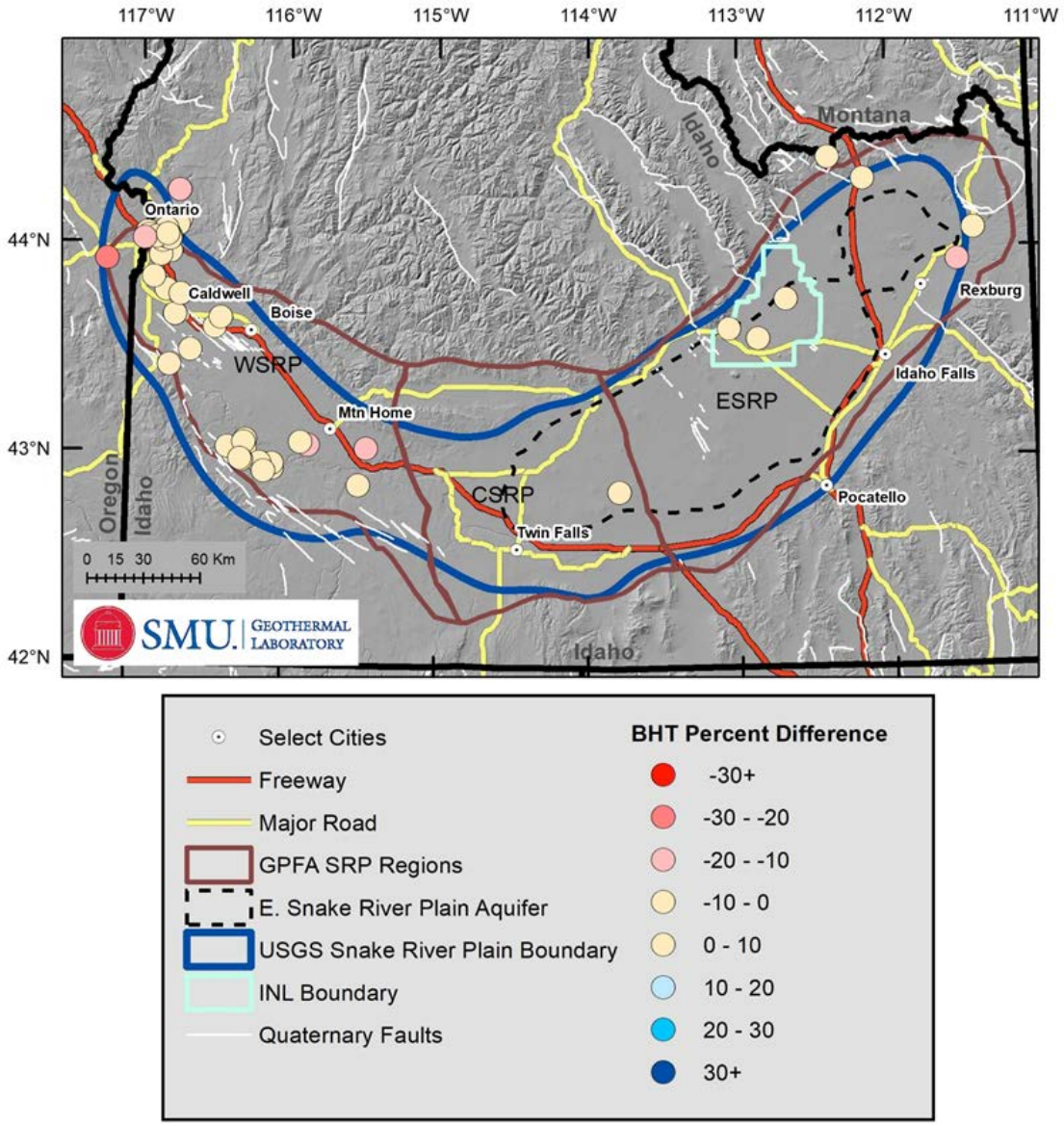

Figure 10. Percent difference of calculated BHT minus observed BHT. The model underpredicts observed temperature where there are negative percent difference values and overpredicts temperature where there are positive percent difference values.

4.1 Western Snake River Plain

Many of the new data are BHT derived heat flow in the WSRP. The new data generally agree with previous heat flow and temperature estimations but contain additional variability because of the higher number of values (Figure 11). The average for new WSRP heat flow values is lower than previous studies, 88 ±19 mW/m² for this study compared to 99 ±4 mW/m² in Blackwell (1989). The lower heat flow average for new data is expected because new data are focused in the central, deeper sedimentary sections of the WSRP. Blackwell (1989) observed the same lower heat flow trend from shallow temperature log data collected in the 1970's and 1980's throughout the central WSRP. There are several high temperature zones within the WSRP. Most of these are along the margins, similar to previous studies and additional high temperature anomalies along the central axis of the WSRP running between Mountain Home and Caldwell. Additional data east of Ontario supports the elevated geothermal gradient and heat flow first seen in the ORE-IDA No. 1 well. One variation between the new map and previous works are the heat flow and temperature estimations along the southwestern margin, near the Owyhee Plateau. New data show one high heat flow region in between low heat flow regions. These three zones within the Quaternary SRP bounding fault zone (Figure 11). While all data used to create this map are considered representative of the regional thermal regime, this complex thermal pattern may be the result of regional fluid flow that is not easily detected within BHT derived heat flow values.

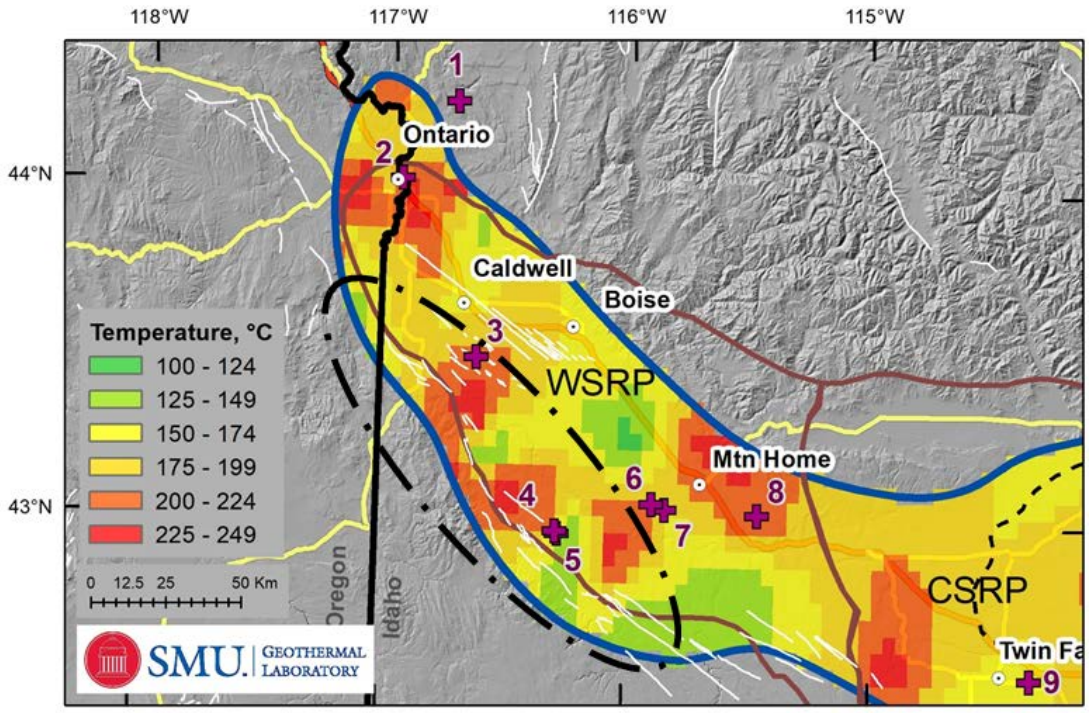

Figure 11. Temperature at 4 km depth in the Western Snake River Plain. The complex thermal signature, potentially related to fluid flow along faults, is highlighted along the southern margin (black dashed oval).

4.2 Estimated Electrical Potential

Electrical potential is estimated following the same procedure as Frone et al. (2015) (Table 4), which is from Augustine (2011). The calculation is for volume of 1 km centered at each kilometer depth interval. NREL defined non-development areas are removed. Our new estimates suggest there are ~44,000 MW_e of EGS electrical potential within the SRP to 4 km. This is assuming a 20% recovery factor. Many of the energy estimates are from the 3 and 4 km depths and in the 150 – 225 °C range, although there are some estimates of electrical potential in the 2 km depth range. The 2 km high resource potential region near Mountain Home is based on well control with temperatures of 127 – 140 °C and 188 °C at 1600 – 1900 m and 2712 m, respectively. The high estimated temperature at 2 km along the southern margin of the SRP, between Pocatello and Twin Falls, does not have deep temperature control and is considered less constrained and therefore a higher risk area for exploration.

Table 4. Estimated electrical power production for the Snake River Plain

Temperature Interval , °C	**MW_e per Depth, km**				**Total Potential MW_e**
	1	**2**	**3**	**4**	
150 - 175		109	10,213	7,814	**18,136**
175 - 200			2,708	12,139	**14,846**
200 - 225			281	7,725	**8,006**
225 - 250				2,434	**2,434**
250 - 275				371	**371**
275 - 300					
Totals	**0**	**109**	**13,202**	**30,482**	**43,793**

Previous national-scale EGS electrical potential estimates were made for 3.5 - 10 km depths utilizing the Blackwell and Richards (2004) Geothermal Map of North America and following a similar calculation methodology (Tester et al., 2006; Augustine, 2011; Augustine, 2016). This detailed approach results in larger EGS energy potential for the SRP compared to previous assessments performed by Blackwell et al. (2011b). Using the same SRP boundary, the 2011 3.5 km temperature-at-depth Map of the United States produces an EGS energy potential of approximately 13,800 MW_e; in contrast, this study predicts EGS energy potential of approximately 24,500 MW_e, or a 75% increase in electrical potential (Table 5). Here, the 1 km volume is centered at 3.5 km. The power potential is greater for the new map because of increased temperatures within the WSRP, which is a result of the increase in data density and removal of shallow wells. Much of the ESRP, however, has lower electricity potential because the systematic addition of the ESPRA has decreased the temperature estimates within the thickest part of the aquifer.

Table 5. Estimated power potential comparison for the Snake River Plain at 3.5 km depth.

Temperature Interval , °C	2011 Map	This Study
150 - 175	13,353	12,939
175 - 200	425	8,159
200 - 225		3,043
225 - 250		351
250 - 275		
275 - 300		
Totals	**13,778**	**24,492**

5. Discussion

5.1 Model Parameters and Potential Error

Several model parameters are poorly defined, which increases uncertainty in heat flow and temperature-at-depth estimates. The model parameters, data examination, and potential error are examined more thoroughly in the companion poster (Batir et al., 2020a). A brief explanation of the largest unknowns, handling of these unknowns, and potential error in the extrapolations, are discussed here.

5.2.1 Heat Flow Error sources

The highest quality heat flow values derived from equilibrium temperature logs and accompanying thermal conductivity measurements have less than 10% measurement error. This value is based on equilibrium temperature logs collected by SMU with an accuracy of ±0.01 °C (Blackwell and Spafford, 1987) and thermal conductivity on the divided bar having an accuracy of approximately 5% error. Measurement error, however, does not account for the potential systemic error propagation from improperly interpreted data. Shallow temperature logs that do not fully penetrate an aquifer could appear conductive, exhibiting a linear gradient to the bottom depth. This area may in fact be purely conductive because it is a low permeable section above an aquifer, however, it could be anomalously warmed or cooled from the underlying aquifer not visible in the temperature log. Data with obvious advective heat flow signatures are removed during data evaluation, but there could still be these data with less obvious advective flow and unrepresentative heat flow, especially in the medium depth data. Evaluating these linear well logs for advective heat flow is problematic and requires further research.

Error in BHT derived heat flow values are from both the geothermal gradient and the thermal conductivity estimation. Geothermal gradients are ±20% accurate based on the compound error from the generalized surface temperature and unequilibrated BHT temperatures (Blackwell et al., 2010). The thermal conductivity values are approximately ±25% accurate based on the accuracy of the two inputs - a stratigraphic column for the well from surface to the depth of BHT and the assigned thermal conductivity for each lithology encountered. The generalized stratigraphic columns are developed from deep wells, which are few and geographically far apart, therefore,

limits the ability to interpolate thinning of basalt layers and stratigraphy changes. For example, the variation of percent sedimentary rocks in upper 2 km within the WSRP generalized stratigraphic column for the Upper Deer Flat 11-19, the J.N. James 1, and the ORE-IDA 1, are 75%, 62%, and 94%, respectively (see columns in Final Report Appendix, Batir et al., 2020b). This small set of deep wells show unknown variability in the stratigraphic column that could propagate approximately ±20% error in the assigned lithology and respective thickness. The important question then becomes: how significant are the stratigraphy changes to a generalized thermal conductivity model? The significance of the stratigraphy depends on the difference in thermal conductivity for the two primary stratigraphic rocks, the sedimentary section versus the basalt.

Thermal conductivity is measured for basalt throughout the SRP, but only in a few locations for sedimentary rocks, in wells associated with the Vale geothermal anomaly and the ORE-IDA 1 well. The sedimentary rock average is 1.8 ±0.4 W/m*K with a range from 1.1 to 2.65 W/m*K (*n =18*). The basalt average is 1.8 ±0.3 W/m*K with a range of 1.1 to 2.3 W/m*K (*n = 28*), but also shows a clear decrease in thermal conductivity with increasing depth. Although there is a low sample count for thermal conductivity measurements, these similar thermal conductivity values regardless of rock type suggests error should be approximately ±25%, the standard deviation of the measured values.

5.2.2 Temperature-at-Depth Error Sources

The largest unknown input for the entire SRP is the crustal structure of the upper 10 – 20 km, specifically for estimating upper crust thickness and the heat generation. Upper crustal felsic rocks produce the majority of radiogenic heat production within the Earth and are the basis for the heat flow versus heat production, the Q-A relationship, utilized in this study (see Methods section for details). There is not an established Q-A relationship for the SRP, rather the original Q-A relationship (Roy et al., 1968) is assumed accurate for estimating the radiogenic heat production component of terrestrial heat flow. As explained in the methodology, the thickness of the heat producing layer, *b*, is assumed to be 7.5 ±2.5 km based on recent seismic interpretations (Harper, 2018) and A is calculated for each individual well to satisfy the Q-A relationship. Previous estimates of the thickness of the upper crust range from 0 – 10 km depending on the study and location in the SRP (Hill and Pakiser, 1967; Sparlin, 1981). These values were used in previous SRP thermal modeling (Brott et al., 1978; Brott et al., 1981; Blackwell, 1989; Blackwell et al., 1992). To understand the impact of basement depth, both *b* = 7.5 and 10 km are used for this study. The 4 km temperatures varied by ± 7 °C (hotter for b = 10 km), equivalent to a maximum of 6% error due to *b* thickness.

The radiogenic heat production of the upper crust, A, is another unknown. In this study, the values of A range from 0 to 15 $\mu W/m^3$ with an average 5.3 ±4.3 $\mu W/m^3$ in the model, in order to satisfy the Q-A relationship. Calculated A values from a worldwide dataset of whole rock geochemistry of igneous rocks range from 0 – 11 $\mu W/m^3$ (Hasterok and Webb, 2017) and range from 0 – 4.5 $\mu W/m^3$ with an average of 3.2 ±0.8 $\mu W/m^3$ for whole rock geochemistry samples in the SRP (Hildreth et al., 1991; Troch et al., 2017; Colón, 2018). The current thermal model is over-estimating heat production. Two ways to make the modeled A value match the calculated A from rock samples is: 1) increase *b*, which redistributes the heat production to deeper parts of the crust, or 2) have an additional heat source such as advection or higher basal heat flow. Seismic

data do not support a thicker *b* layer, which suggests heat in the SRP could be coming from either basal heat flow or an advective heat source.

5.2 Comparison with Previous Work

Recent studies in the SRP include the Geothermal Play Fairway Analysis (GPFA) (DeAngelo et al., 2016), a FORGE site feasibility study (Podgorney et al., 2016), and the SMU Geothermal Laboratory Heat Flow Map of the Conterminous United States (Blackwell et al., 2011). Both the GPFA and FORGE projects utilized the Blackwell et al. (2011) results as the primary or one of the primary heat flow datasets to assess temperature and thermal energy potential. The GPFA went beyond heat flow by incorporating multiple heat source indicators to their heat favorability map (DeAngelo et al., 2016). The GPFA, counterintuitively, did not find a direct relationship between geothermal potential and proximity of the current Yellowstone Hotspot location. That can be explained by the variety of different indicators used in the GPFA beyond well heat flow, e.g., volcanic vents distribution, groundwater temperature, and He isotope composition and geothermometry of hot spring and well waters (Shervais et al., 2020). The 2011 SMU Geothermal Laboratory Heat Flow Map of the Conterminous United States utilized wellbore data when available, and contour control points based on geology where heat flow measurements were not available, similar to the expert-driven weighting approach utilized for the GPFA (DeAngelo et al., 2016). The 2011 SMU temperature maps shows the expected direct relationship of thermal energy potential to the proximity to the Yellowstone Hotspot, east of the northeastern terminus of the SRP. The newest heat flow map is similar to the 2011 SMU heat flow map in that they show a loose correlation between proximity to the Yellowstone Hotspot and geothermal potential. With that said, there continues to be a discussion as to how much heat is still retained in the rocks from past and any present hotspot activity. The 2020 temperature-at-depth maps show the ESRP with cooler temperatures and the localized high temperatures could merely be from misinterpreted advective fluid flow along deep faults. These shallow high temperatures make the sites possible targets for geothermal resource projects based on reduced drilling expense.

Comparing the new 3.5 km SMU temperature map (Figure 2b) with the 2011 map (Figure 2a), the new map differs in that the model utilizes the bottom depth of the ESRPA as the upper thermal boundary condition in the ESRP, thereby producing more variability in the temperatures. A large portion of the ESRP is now modeled to be below the EGS temperature cutoff of 150 °C. This new lower temperature estimate is driven by addition of the ESRPA in conjunction with several lower heat flow values. For the WSRP the new 3.5 km temperature map is also more variable from the increased data and an updated thermal conductivity model. With the changes in the modeling, there is increased ability to compare results with complementary geophysical data. Still, geophysical studies cannot predict temperature at depths below 4 km, so drilling wells and measuring downhole temperature is the only way to truly validate the heat flow models.

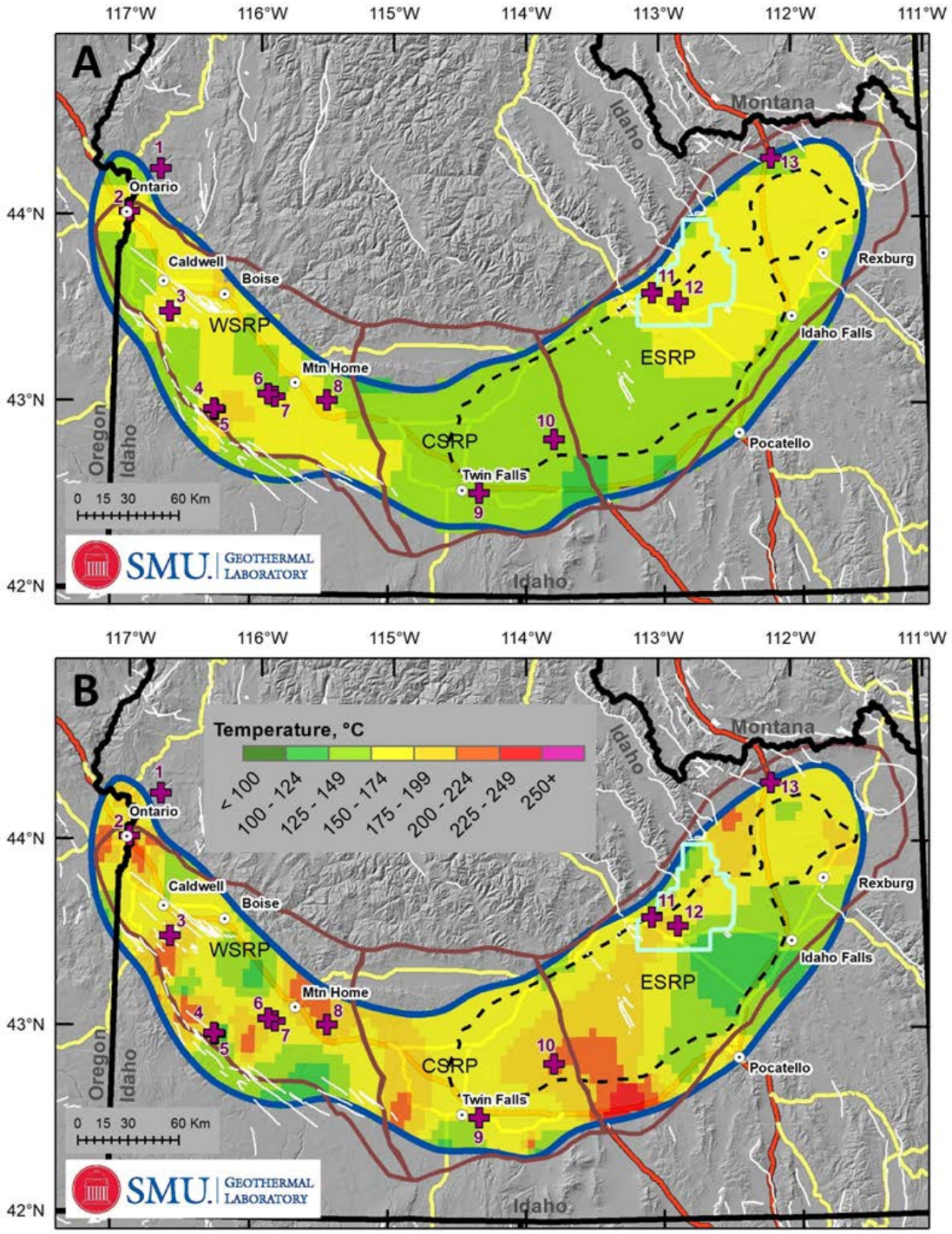

Figure 12: (A) 2011 SMU temperature-at-depth map at 3.5 km (Blackwell et al., 2011b). (B) New temperature-at-depth map at 3.5 km produced for this study.

5.3 Additional Thoughts

The early eruptions of the SRP are felsic so the geologic section is characteristically younger basalt over rhyolite or sediments and rhyolite on the margins, particularly the southern margins. Felsic/rhyolitic volcanic rocks typically are low in permeability except where fractured. The opposite is true for mafic/basaltic volcanic rocks where thin lava flow sequences are highly porous along their flow surfaces making them excellent aquifers. Yet, fluid flow in these felsic rocks is as pervasive as the young, unaltered basalts above them and along the margins. Thus, the temperatures of the felsic sections tend to also be isothermal from fluid flow, as are the basalt sections. The main difference between the felsic and basalt fluid flow within the SRP is that the felsic sections are often capped by sedimentary rocks, which decreases hydrological communication with the surface. This decreased hydrological communication and regional dip of felsic units toward the center of the SRP produces an elevated thermal regime in the center with a shallow to slightly artesian water table characterized by isothermal temperature profiles that range from 30 to 80 °C for the upper 1500 m.

This phenomenon is visible in the CSRP where felsic rocks contain isothermal sections several thousand feet thick as demonstrated in the Kimberly well and in the deep Grandview area wells (Blackwell et al., 1992; Utah State University, 2014b). In the ESRP, it is the basalts that form the aquifer, creating isothermal temperature profiles, although the temperatures in the ESRP are at or near shallow groundwater temperatures, ranging from 9 to 20 °C to 1200 m (McLing et al., 2016; Lachmar et al., 2017). This is less visible within the WSRP because of the thicker sedimentary section. These typical fluid flow characteristics of the basalt and rhyolite sections make geothermal assessment of the SRP regional area more difficult since wells deeper than 1.5 km or more are necessary to fully determine crustal thermal regimes. Thus, the few deep wells that do exist take on particularly important meaning for geothermal assessment despite their significant spatial separation.

For the modeling to calculate temperatures-at-depth, the heat flow versus radiogenic heat production (Q-A relationship) is an over-simplification of the total terrestrial heat flow for the SRP. The A value outputs from the thermal model for certain wells requires either a higher radiogenic heat production than what whole rock geochemistry suggests (0 – 4.5 $\mu W/m^3$) or a thicker crust than what seismic studies for the area indicate (0 – 8 km). In order for the observed heat flow values to agree with whole rock geochemistry and seismic derived upper crustal thickness, the observed heat flow requires an additional heat component such as higher mantle heat flow, advective heat transfer within the crust (faults), basin wide heat refraction, or a combination of all. As an example, the Kimama well has a 123 mW/m^2 heat flow. If mantle heat flow is 60, then 63 mW/m^2 heat must be coming from radiogenic heat production? That would require 6.3 $\mu W/m^3$ of heat production and 10 km of heat producing crust – neither of which fits the whole rock geochemistry estimates or crustal thickness estimates from seismic studies.

The work presented here focuses on direct, depth-correlated measurements to estimate heat flux and temperatures, although there are other potential temperature indicators used in the GPFA that could add insight and confidence to our estimates (Shervais et al., 2015; Shervais et al., 2020). Collecting geothermometry of produced fluids from the high temperature areas could be used to test the plausibility of these modeled temperatures. A spatial correlation of hot spring and ground water temperatures to nearby wells could help find shallow or isolated isothermal aquifers.

Volcanic vents are another potential indicator of heat, although it is still unclear if there is enough known about each vent to quantify these heat sources.

5.4 Suggested Next Steps

Additional data collection is necessary to further refine assumptions in this model and to resolve remaining questions. Below is a list of suggested future studies, with descriptions of how each would aid in geothermal exploration and thermal regime modeling.

1) New seismic studies that focus on mapping the location and thickness of upper crust in the SRP would reduce the uncertainty in the utilized *b* value and produce more understanding of the Q-A relationship of the SRP, if this is a valid and applicable relationship for this region.
2) Deep drilling in the ESRP that completely penetrates below the ESRPA, records a linear (conductive) gradient for at least 100 m, and possibly drills into the felsic rocks. Such a well would increase heat flow and basement knowledge in a region that lacks sufficient data coverage because of the expansive ESRPA. Suggested well locations are along the south and/or east margin of the ESRPA, such as between Pocatello and Idaho Falls or northwest of Rexburg.
3) Deep wells both northwest and northeast of Rexburg would also increase understanding of lithospheric cooling along the Yellowstone Hotspot track that would aid in large-scale time-dependent, volcanism age driven thermal regime models.
4) To the north of the SRP, outside this project focus, is the Central Idaho Basin and Range. This area was cited by Blackwell (1989) as a potential geothermal resource zone, yet no additional data collection or analysis were ever completed. With the focus on EGS and new interest in sedimentary basins for geothermal EGS, this region continues to be a possible area for exploration.

6. Conclusions

This study produced increased resolution of the thermal regime of the WSRP and a better understanding of the thermal regime controls in the greater SRP region. While limited new well data are available for the CSRP and ESRP regions, the additional well data coverage for WSRP allows for at least one data point within any ~15 km gridding radius circle. Comparing the geothermal resource evaluation work from the 1970's and 1980's, it is surprising to see many areas with high temperature wells still not included in assessments by government or private exploration. The areas along the edges of the SRP are complicated, with fault-related fluid flow and complex crustal structure, yet are prospective for both conventional geothermal (power and direct use) and EGS development. The elephant in the room, the ESRPA, is modeled with a high heat source below, yet until additional wells penetrate to depths below 1 km, the proportion of that heat being advectively carried away by the aquifer will remain unknown, along with the full geothermal resource potential. The thermal potential results from this study show electricity potential (≥150°C) within the 1 km to 4 km depths as approximately 44,000 MW_e. At the 3.5 km depth, power potential is 75% greater based on the new temperature-at-depth maps compared to the same area within the SMU 2011 temperature U.S. map, even with the removal of the area within the ESRPA.

Acknowledgements

This paper includes research contributions from Christine Ferguson and Sharon Fields who work with the authors in the SMU Geothermal Laboratory. The work was performed in collaboration with the National Renewable Energy Laboratory, upon funding from the Alliance for Sustainable Energy, LLC, Managing and Operating Contractor for the National Renewable Energy Laboratory for the U.S. Department of Energy, under Subcontract NO. XEJ-9-92239-01 under prime Contract NO. DE-AC36-08GO28308, and the Bureau of Land Management (BLM) under Interagency Agreement (IAA) L16PG00068/P0003. The views expressed in the article do not necessarily represent the views of the NREL or the U.S. Government. The U.S. Government retains and the publisher, by accepting the article for publication, acknowledges that the U.S. Government retains a nonexclusive, paid-up, irrevocable, worldwide license to publish or reproduce the published form of this work, or allow others to do so, for U.S. Government purposes.

REFERENCES

Augustine, Chad. *Updated US Geothermal Supply Characterization and Representation for Market Penetration Model Input*. No. NREL/TP-6A2-47459. National Renewable Energy Lab. (NREL), Golden, CO, United States, 2011

Augustine, Chad. *Update to Enhanced Geothermal System Resource Potential Estimate*. United States. 2016. Online at: https://www.osti.gov/servlets/purl/1330935

Bargar, Keith E., and Terry EC Keith. *Hydrothermal mineralogy of core from geothermal drill holes at Newberry volcano, Oregon*. No. 1578. US Geological Survey, 1999.

Batir, Joseph; Maria Richards, Matthew Hornbach, David Blackwell, Amanda Kolker. Uncertainty Analysis of Subsurface Temperature Estimates in the Snake River Plain, Idaho. *Geothermal Resources Council Trans*., Abstract and Poster, 2020a

Batir, Joseph; Maria Richards, Matthew Hornbach, David Blackwell. Final Report to Bureau of Land Management on the Shallow EGS Potential of the Snake River Plain under Subcontract NO. XEJ-9-92239-01 under prime Contract NO. DE-AC36-08GO28308 of the Alliance for Sustainable Energy, LLC, Managing and Operating Contractor for the National Renewable Energy Laboratory, 2020b.

Blackwell, D.D. Heat flow determinations in the northwestern United States, *J. Geophys. Res*., 74, 992-1007, 1969.

Blackwell, D.D. The thermal structure of the continental crust, in *The Structure and Physical Properties of the Earth's Crust, Geophys. Mono. Ser. 14*, ed. J.G. Heacock, 169-184, AGU, Washington D.C., 1971.

Blackwell, David. Regional implications of heat flow of the Snake River Plain, northwestern United States. *Tectonophysics*, 164, 323-344, 1989.

Blackwell, D.D.; J.L. Steele, S. Kelley, M.A. Korosec. Heat flow in the State of Washington and thermal conditions in the Cascade Range *J. Geophys. Res*., 95, 19495-19516, 1990.

Blackwell, David D.; Shari Kelley, John L. Steele. Heat flow modeling of the Snake River Plain, Idaho. *US Department of Energy Report for contract DE-AC07-761DO1570,* 109 p., 1992.

Blackwell, D.D., and M. Richards. Geothermal Map of North America, *American Association of Petroleum Geologists* Map, scale 1:6,500,000, Product Code 423, 2004a.

Blackwell, D.D., and M. Richards. The 2004 Geothermal Map of North America; Explanation of Resources and Applications, *Geothermal Resources Council Trans*., 28, 317-320, 2004b.

Blackwell, David D.; Petru T. Negraru, Maria C. Richards. Assessment of the enhanced geothermal system resource base of the United States. *Natural Resources Research* 15, no. 4, 283-308 2006.

Blackwell, David; Patrick Stepp, Maria Richards. Comparison and discussion of the 6 km temperature maps of the western US prepared by the SMU Geothermal Lab and the USGS. *GRC Transactions* 34, GRC1028696, 2010.

Blackwell, D.D.; M.C. Richards, Z.S. Frone, J.F. Batir, M.A. Williams, A.A. Ruzo, R.K. Dingwall. *SMU Geothermal Laboratory Heat Flow Map of the Conterminous United States*, U.S. Copyright VA 0001377160, 2011a. Supported by Google.org. Online at: http://www.smu.edu/geothermal.

Blackwell, David; M. Richards, Z. Frone, J. Batir, A. Ruzo, R. Dingwall, M. Williams. Temperature-at-depth maps for the conterminous United States and geothermal resource estimates, *Geothermal Resources Council Transactions*, v. 35, 2011b.

Bonnichsen, Bill, and M.M. Godchaux. Late Miocene, Pliocene, and Pleistocene geology of southwestern Idaho with emphasis on basalts in the Bruneau-Jarbidge, Twin Falls, and western Snake River Plain regions. *Tectonic and Magmatic Evolution of the Snake River Plain Volcanic Province:* Idaho Geological Survey Bulletin, 30, 233-312, 2002.

Brott, C.A.; D.D. Blackwell, J.C. Mitchell. Heat flow in the Snake River Plain region, southern Idaho, *Idaho Dept. Water Resour. Water Info. Bull.*, 30, Part 8, 195 pp., 1976.

Brott, C.A.; D.D. Blackwell, J.C. Mitchell. Tectonic implications of the heat flow of the western Snake River Plain, Idaho, *Idaho Dept. Water Resources Water Inf. Bull. 30*, pt. 8, 195 pp, 1978.

Brott, C.A.; D.D. Blackwell, J.P. Ziagos. Thermal and tectonic implications of heat flow in the Eastern Snake River Plain, *J. Geophysical Research*, 86, 11709-11734, 1981.

DeAngelo, Jacob; John W. Shervais, Jonathan M. Glen, Dennis L. Nielson, Sabodh Garg, Patrick Dobson, Erika Gasperikova *et al*. GIS methodology for geothermal play fairway analysis: Example from the Snake River Plain volcanic province. In *Proceedings 41st Workshop on Geothermal Reservoir Engineering,* Stanford University, 2016.

Frone, Zachary; Maria Richards, David Blackwell, Chad Augustine. Shallow EGS Resource Potential Maps of the Cascades. In *Proceedings 40th Workshop on Geothermal Reservoir Engineering,* Stanford University. *SGP-TR-19,* 2015.

Gass, T.E. Geothermal heat pumps, Geothermal Resources Council Bulletin, 11, 3-8, 1982.

Glen, Jonathan MG; Lee Liberty, Erika Gasperikova, Drew Siler, J.W. Shervais, Brent Ritzinger, Noah Athens, Tait Earney. Geophysical investigations and structural framework of

geothermal systems in west and southcentral Idaho: Camas Prairie to Mountain Home. In *Proceedings of the 42nd Workshop on Geothermal Reservoir Engineering*, Stanford University, 1021-33, 2017.

Glen, J.M.G.; L. Liberty, J. Peacock, E. Gasperikova, T. Earney, W. Schermerhorn, D. Siler, J. Shervais, P. Dobson. A geophysical characterization of the structural framework of the Camas Prairie geothermal system, southcentral Idaho. *Geothermal Resources Council Transactions* 42, 466–481, 2018.

Hasterok, D. and J. Webb. On the radiogenic heat production of igneous rocks. *Geoscience Frontiers*, vol. 8, 919-940, 2017. Online at: https://doi.org/10.1016/j.gsf.2017.03.006

Harper, Thomas Branson. *Crustal composition beneath southern Idaho: Insights from teleseismic receiver functions*. Masters of Science Thesis at Boise State University, 98 p., 2018.

Hill, D.P. and L.C. Pakiser. Seismic-refraction study of crustal structure between the Nevada Test Site and Boise, Idaho. *Geological Society of America Bulletin* 78, no. 6, 685-704, 1967.

Jordan, Teresa E.; Maria C. Richards, Franklin G. Horowitz, Erin Camp, Jared D. Smith, Calvin A. Whealton, Jery R. Stedinger, Matthew J. Hornbach, Zachary S. Frone, Jefferson W. Tester, Brian Anderson, Kelydra Welcker, Catherine Chickering Pace, Xiaoning He, Maria Beatrice Magnani, Rahmi Bolat. *Low Temperature Geothermal Play Fairway Analysis For The Appalachian Basin: Phase 1 Revised Report*, November 18, 2016. Online at doi:10.2172/1341349. https://www.osti.gov/servlets/purl/1341349.

Lachenbruch, Arthur H. Preliminary geothermal model of the Sierra Nevada. *Journal of Geophysical Research* 73, no. 22, 6977-6989, 1968.

Lachmar, TE; TG Freeman, CJ Sant, JR Walker, JF Batir, JW Shervais, JP Evans, DL Nielson, DD Blackwell. Effect of an 860-m thick, cold, freshwater aquifer on geothermal potential along the axis of the eastern Snake River Plain, Idaho. *Geothermal Energy,* 5:28, 2017. Online at doi:10.1186/s40517‐017‐0086‐8.

Lachmar, T.E.; Freeman, T.G., Kessler, J.A., Batir, J.F., Evans, J.P., Nielson, D.L., Shervais, J.W., Chen, X., Schmitt, D.R., Blackwell, D.D. Evaluation of the geothermal potential of the western Snake River Plain based on a deep corehole on the Mountain Home AFB near Mountain Home, Idaho. Geothermal Energy 7, 26, 2019. Online at doi:10.1186/s40517-019-0142-7.

Lindholm, Gerald F. *Summary of the Snake River Plain regional aquifer-system analysis in Idaho and eastern Oregon*. No. 1408-A. US Government Printing Office, 1996.

Ludington, S.; B.C. Moring, R.J. Miller, J.G. Evans, P.S. Stone, A.A. Bookstrom, C.J. Nutt, D.R. Bedford, G.A. Haxel, M.J. Hopkins, K.S. Flynn. Preliminary integrated geologic map databases for the United States - Western States - California, Nevada, Arizona, Washington, Oregon, Idaho, and Utah, 2005. Online at http://pubs.usgs.gov/of/2005/1305/.

Machette, M.N.; K.M. Haller, R.L. Dart, S.B. Rhea. Quaternary fault and fold database of the United States: *U.S. Geological Survey Open-File Report 03-417*, 2003. Online at http://qfaults.cr.usgs.gov/faults/.

McLing, Travis L.; Richard P. Smith, Robert W. Smith, David D. Blackwell, Robert C. Roback, Andrus J. Sondrup. Wellbore and groundwater temperature distribution eastern Snake River

Plain, Idaho: Implications for groundwater flow and geothermal potential. *Journal of Volcanology and Geothermal Research* 320, 144-155, 2016.

McCurry, M.; T. McLing, R.P. Smith, W.R. Hackett, R. Goldsby, W. Lochridge, R. Podgorney, T. Wood, D. Pearson, J. Welhan, M. Plummer. Geologic Setting of the Idaho National Laboratory Geothermal Resource Research Area. In *Proceedings, 41st Workshop on Geothermal Reservoir Engineering: Stanford University, Stanford California, SGP-TR-209,* 2016.

NGDS National Geothermal Data System, SMU Node, 2014. Online at: geothermal.smu.edu/GTDA

Pierce, Kenneth L. and Lisa A. Morgan. Is the track of the Yellowstone hotspot driven by a deep mantle plume?—Review of volcanism, faulting, and uplift in light of new data. *Journal of Volcanology and Geothermal Research* 188, no. 1-3, 1-25, 2009.

Podgorney, R.; Neil Snyder, M. Roy. A Snake River Plain Field Laboratory for Enhanced Geothermal Systems: an Overview of the Snake River Geothermal Consortium's Proposed FORGE Approach and Site. In *Proceedings, 41st Workshop on Geothermal Reservoir Engineering*, Stanford University, 2016.

Rodgers, David W.; H. Thomas Ore, Robert T. Bobo, Nadine McQuarrie, Nick Zentner, B. Bonnichsen, C. M. White, M. McCurry. Extension and subsidence of the eastern Snake River Plain, Idaho. *Tectonic and Magmatic Evolution of the Snake River Plain Volcanic Province: Idaho Geological Survey Bulletin* 30, 121-155, 2002.

Roy, Robert F.; David D. Blackwell, Francis Birch. Heat generation of plutonic rocks and continental heat flow provinces. *Earth and Planetary Science Letters* 5, 1-12, 1968.

Shervais, John W.; Gaurav Shroff, Scott K. Vetter, Scott Matthews, Barry B. Hanan, James J. McGee. *"Origin and Evolution of the Western Snake River Plain: Implications for Stratigraphy, Faulting, and the Geochemistry of Basalts Near Mountain Home, Idaho: Idaho Geological Survey Bulletin*, 2002.

Shervais, John W., *et al.* "Hotspot: The Snake River Geothermal Drilling Project – Initial Report." *Geothermal Resources Council Transactions* 36, 767-772, 2012.

Shervais, John W.; Douglas R. Schmitt, Dennis Nielson, James P. Evans, Eric H. Christiansen, Lisa Morgan, W. C. Shanks *et al*. First results from HOTSPOT: the Snake River Plain scientific drilling project, Idaho, USA. *Scientific Drilling* 15, 2013.

Shervais, John W.; Jonathan M. Glen, Lee M. Liberty, Patrick Dobson, Erika Gasperikova, Eric Sonnenthal, Charles Visser *et al*. Snake River Plain Play Fairway Analysis–Phase 1 Report. *Geothermal Resources Council Transactions* 39, 761-769, 2015.

Shervais, John W.; Jonathan M. Glen, Drew Siler, Lee M. Liberty, Dennis Nielson, Sabodh Garg, Patrick Dobson *et al*. Play Fairway Analysis in Geothermal Exploration: The Snake River Plain Volcanic Province. In *Proceedings, 45st Workshop on Geothermal Reservoir Engineering*, Stanford University, 2020.

Smith, Jared. *Analytical and geostatistical heat flow modeling for geothermal resource reconnaissance applied in the Appalachian Basin*. PhD Dissertation, Cornell University, Ithaca, NY, 2016.

Smith, J., and F. Horowitz. Seismic Risk Map Creation Methods. *Low Temperature Geothermal Play Fairway Analysis for the Appalachian Basin: Final Phase 1 Research Report*. US Dept. of Energy, DEE0006726, 2016.

Sparlin, M. A. *Crustal structure of the eastern Snake River Plain determined from ray-trace modeling of seismic refraction data*, M.S. Thesis, 62 pp., Purdue Univ., W. Lafayette, Ind., 1981.

Stutz, George R.; Mitchell Williams, Zachary Frone, Timothy J. Reber, David Blackwell, Teresa Jordan, Jefferson W. Tester. A well by well method for estimating surface heat flow for regional geothermal resource assessment. In *Proceedings, 37th Workshop on Geothermal Reservoir Engineering*, Stanford University. *SGP-TR-194*, 2012.

Tester, J. W.; B. Anderson, A. Batchelor, D. Blackwell, R. DiPippo, E. Drake, J. Garnish, B. Livesay, M.C. Moore, K. Nichols, S. Petty, N. Toksoz, R. Veatch, C. Augustine, R. Baria, E. Murphy, P. Negraru, M. Richards. *The future of geothermal energy: Impact of enhanced geothermal systems EGS on the United States in the 21st Century*. Massachusetts Institute of Technology, DOE Contract DE-AC07-05ID14517 Final Report, 374 p., 2006.

U.S. Geological Survey. *Snake River Plain Basin-fill aquifer system*, vector digital data, 2nd Edition: Reston, VA, 2015. Online at: https://water.usgs.gov/GIS/metadata/usgswrd/XML/snake_river_plain_aquifer_system.xml#stdorder

Utah State University. Project HOTSPOT: Kimama Well Borehole Geophysics Database, 2014a. Online at: http://gdr.openei.org/submissions/291

Utah State University. Project HOTSPOT: Kimberly Well Borehole Geophysics Database, 2014b. Online at: http://gdr.openei.org/submissions/283

Utah State University. Project HOTSPOT: Mountain Home Well Borehole Geophysics Database, 2014c. Online at: http://gdr.openei.org/submissions/284

Whitehead, R.L. Geohydrologic framework of the Snake River plain regional aquifer system, Idaho and eastern Oregon. *USGS Professional Paper 1408-B, 1992*. Online at doi: 10.3133/pp1408B

Wood, Spencer H., and Drew M. Clemens. Geologic and tectonic history of the western Snake River Plain, Idaho and Oregon. *Tectonic and Magmatic Evolution of the Snake River Plain Volcanic Province: Idaho Geological Survey Bulletin*, 2002.